

Cooling of hybrid stars with spin down compression *

Miao Kang¹, Xiao-Dong Wang¹ and Na-Na Pan²

¹ College of Physics and Electronics, Henan University, Kaifeng 475004, China;
kangmiao07@gmail.com

² College of Mathematics and Physics, Chongqing University of Posts and Telecommunications,
Chongqing 400065, China

Received 2009 May 15; accepted 2009 August 22

Abstract We study the cooling of hybrid stars coupled with spin-down. Due to the spin-down of hybrid stars, the interior density continuously increases and different neutrino reactions may be triggered (from the modified Urca process to the quark and nucleon direct Urca process) at different stages of evolution. We calculate the rate of neutrino emissivity of different reactions and simulate the cooling curves of the rotational hybrid stars. The results show that the cooling curves of hybrid stars clearly depend on a magnetic field if the direct Urca reactions occur during the spin-down. Comparing the results of the rotational star model with the transitional static model, we find the cooling behavior of the rotational model is more complicated; the temperature of the star is higher, especially when direct Urca reactions appear in the process of rotation. Then, we find that the predicted temperatures of some rotating hybrid stars are compatible with the pulsar's data which are in contradiction with the results of the transitional method.

Key words: dense matter — stars: rotation — equation of state

1 INTRODUCTION

The interior of neutron stars contains matter beyond the nuclear saturation density which we have not yet seen. The cooling of neutron stars gives us an important tool to study the properties of such dense matter. The traditional investigations of cooling often adopt the static star model which is not connected with spin-down. It is well known that neutron stars would spin-down due to magnetic dipole radiation. The spin-down compression of stars may lead to the changes in chemical composition (from nucleon matter to deconfined quark matter) and structure (mixed phase and quark phase appearing). The coupling of cooling and spin-down correlates stellar surface temperatures with rotational state as well as with time. The interlinked processes of spin-down and cooling present intriguing prospects to gain insight into the fundamental properties of dense matter in neutron stars by confronting them with thermal emission data from observations (Stejner et al. 2008; Page et al. 2006; Yakovlev & Pethick 2004).

Neutron stars are born with temperatures above 10^{10} K. The dominant cooling mechanism of stars is the neutrino emission from the interior for the first several thousand years after birth, which can be generated via numerous reactions (Yakovlev & Pethick 2004). The nucleon direct Urca (NDU) reaction, the most efficient one, is only possible if the fraction of protons exceeds a certain threshold. It is impossible to satisfy the conservation of momentum unless the proton fraction exceeds the value where both

* Supported by the National Natural Science Foundation of China.

the charge neutrality and the triangle inequality can be observed (Lattimer et al. 1991). Hence, the traditional investigations of neutron stars often divide the cooling process into two regimes that are slow and fast cooling due to slow and fast neutrino emission, respectively. Slow cooling occurs in the low mass stars via neutrino emission produced mainly by the nucleon modified Urca (NMU) process. The fast cooling occurs in stars with critical mass M_D (it is of course model dependent) via the NDU process. Comparing with the observed data, we can see that the fast cooling process would result in a contradiction between the predicted temperatures of stars and the observations, which presents a challenge to the traditional model (Page et al. 2006).

The neutron stars containing quark matter are called hybrid stars. Hybrid stars have a more complicated interior structure and matter composition than the pure neutron stars. Due to spin-down compression, the interior density gradually increases and some of the thermodynamic quantities, such as neutrino emission, luminosity and total heat capacity of stars, continuously change with rotational frequency. In particular, the rate of neutrino emission would have an abrupt rise because of direct Urca reactions occurring which would induce the rapid fall of the temperatures of hybrid stars. The appearance of different direct Urca processes can result in different cooling behaviors in the stages of evolution of the stars. The main difference between our model and the traditional model is that our model combines the equation of thermal balance with the rotational star's structure and uses the magnetic dipole radiation model to investigate the changes in thermodynamic quantities and the cooling behavior of hybrid stars with spin frequency as well as with time. The simulations of the cooling curves of rotational stars are more complex than the traditional cases because of the magnetic field dependence and changes of rotational state. Surface temperatures of some stars, including fast cooling processes, are compatible with the pulsar's data due to spin-down.

We take Glendenning's hybrid star model (Glendenning 1997) based on the perturbation theory (Hartle 1967; Chubarian et al. 2000) to study the rotational structure of stars. In our calculation, we only choose the simplest nucleon matter composition, namely neutrons, protons, electrons, and muons, and ignore superfluidity and superconductivity.

2 HYBRID STARS

As the stars spin-down, the nuclear matter is continuously converted into quark matter by the exothermic reactions, i.e. $n \rightarrow u + 2d$, $p \rightarrow 2u + d$, and s quarks immediately appear after weak decay. The deconfinement phase transition put forward by Glendenning (1997, 1992) was the first to indicate the possibility of the occurrence of a mixed phase (MP) of hadron matter and quark matter in a finite density range inside neutron stars. Global charge neutrality of MP can be achieved by a positively charged amount of hadronic matter and a negatively charged amount of quark matter. The Gibbs condition for mechanical and chemical equilibrium at zero temperature between the two phases reads

$$p_{\text{HP}}(\mu_n, \mu_e) = p_{\text{QP}}(\mu_n, \mu_e) = p_{\text{MP}}, \quad (1)$$

where μ_n is the chemical potential of the neutron and μ_e is the chemical potential of the electron. The condition of global charge neutrality in the MP is

$$0 = \frac{Q}{V} = \chi q_{\text{QP}} + (1 - \chi)q_{\text{HP}}, \quad (2)$$

where $\chi = V_Q/V$ is the quark fraction in the MP, thus the energy density ϵ_{MP} of the MP follows as

$$\epsilon_{\text{MP}} = \frac{E}{V} = \chi \epsilon_{\text{QP}} + (1 - \chi)\epsilon_{\text{HP}}. \quad (3)$$

We can obtain the equation of state (EOS) of MP using the above equations. For the hadron part of the star, we adopt the Argonne $V18 + \delta v + U1X^*$ model (Akmal et al. 1998) which is based on the models for the nucleon interaction with the inclusion of a parameterized three-body force and relativistic boost corrections. For the quark matter, we use the EOS of an effective mass bag-model EOS (Schertle et

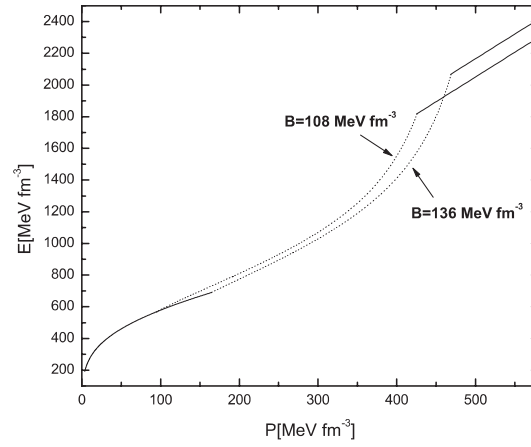


Fig. 1 Model EOS for the pressure of hybrid star matter as a function of the energy density. The hadronic phase EOS is the Argonne $V18 + \delta v + UIX^*$ model. The quark phase is an effective mass MIT bag model with bag constants $B = 136$ and 108 MeV fm^{-3} respectively.

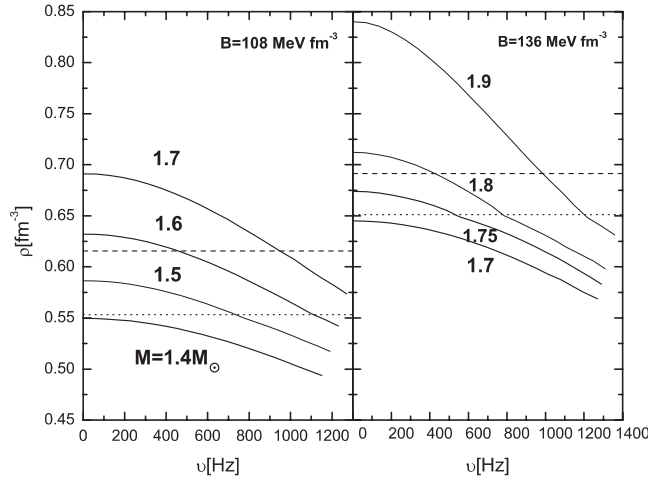


Fig. 2 Central density as a function of rotation frequency for rotating hybrid stars with a different gravitational mass at zero frequency. All sequences have a constant total baryon number. Dotted horizontal lines indicate that deconfined quark matter is produced and dashed horizontal lines indicate that a nucleon direct Urca process is triggered.

al. 1997). In Figure 1, we show the EOS for hybrid stars with deconfinement transition as described above. We choose the parameters for quark matter's EOS with s quark mass $m_s = 150 \text{ MeV}$, a coupling constant $g = 3$ and different bag constants $B = 108 \text{ MeV fm}^{-3}$ and $B = 136 \text{ MeV fm}^{-3}$.

The rotation of stars leads to the change in structure. In the present work, we apply Hartle's approach (Hartle 1967) to investigate the rotational structure of the stars. It is based on the treatment of a rotating star as a perturbation of a non-rotating star, which can be obtained by expanding the metric of an axially symmetric rotating star in even powers of the angular velocity Ω . We assume the frequency of stars at birth is close to the Kepler (mass-shedding limit) frequency (Hartle & Thorne 1968; Latimer et al. 1990; De Araujo et al. 1995). We have shown the central density of rotating stars of different gravitational masses as a function of its rotational frequency in Figure 2. These sequences of star models have the

same total baryon number but a different central density and angular velocity. It is well known that the perturbative approach fails when the angular velocity approaches the mass-shedding limit. However, the rotational frequencies of all known pulsars are much lower than the mass-shedding limit. So, we can use the perturbative theory to investigate the structure of rotating stars unless we are specifically interested in the mass-shedding problem (Benhar et al. 2005). In Figure 2, dotted horizontal lines indicate deconfined quark matter produced and dashed horizontal lines indicate the NDU nucleon direct Urca processes triggered. The appearance of quark matter will result in the occurrence of quark direct Urca (QDU) processes. Such processes are also efficient, but somewhat weaker than the NDU ones. We observe that the spin-down of stars leads to the changes in chemical composition and structure in Figure 2. In the case of bag constant $B = 108 \text{ MeV fm}^{-3}$ (left panel), the quark matter is produced in the interior for the stars with mass $M > 1.4 M_\odot$ (here denote the static mass) in the process of rotation. For an $M = 1.6 M_\odot$ star, for example, a pure neutron star can be transformed into a hybrid star and NDU reactions are triggered during spin-down. It is known that the occurrence of QDU and NDU processes leads to the rapid fall of the temperatures of stars. In Section 4, we discuss in detail how spin-down leads to changes of the temperatures and cooling curves.

3 NEUTRINO EMISSIVITIES

The stellar cooling could be carried out via two channels - neutrino emission from the entire star and thermal emission of photons through the transport of heat from the internal layers to the surface. The emission of neutrinos could carry away energy which would provide efficient cooling for warm neutron stars.

For the hadronic matter, we mainly consider three kinds of processes which are NDU, NMU and nucleon bremsstrahlung (NB). For the quark matter, we take the QDU processes of unpaired quarks, the quark modified Urca (QMU) processes and the quark bremsstrahlung (QB) to be considered. The most powerful neutrino emission is provided by a direct Urca process. The rate of the neutrino emissivity of the NDU processes $n \rightarrow pe\bar{\nu}$, $pe \rightarrow n\nu$ is given by

$$\varepsilon_{\text{NDU}} \simeq 4.0 \times 10^{27} \left(Y_e \frac{\rho}{\rho_s} \right)^{1/3} T_9^6 \Theta_t \text{ erg cm}^{-3} \text{ s}^{-1}, \quad (4)$$

where T_9 is the temperature in units of 10^9 K , $\rho_s = 0.16 \text{ fm}^{-3}$ is the nuclear saturation density, $\Theta_t = \theta(p_{\text{Fe}} + p_{\text{Fe}} - p_{\text{Fn}})$ is the threshold factor, with $\theta(x)$ being 1 for $x > 0$ and 0 otherwise (Lattimer et al. 1991). NDU processes can occur when the fraction of protons exceeds 11%. The presence of muons would raise it to about 15%.

The neutrino emissivity of quark matter has been given firstly by Iwamoto (1982). The QDU processes have been estimated as

$$\varepsilon_{\text{QDU}} \simeq 8.8 \times 10^{26} \alpha_c \left(\frac{\rho}{\rho_s} \right) Y_e^{1/3} T_9^6 \text{ erg cm}^{-3} \text{ s}^{-1} \quad (5)$$

with the standard value of the QCD coupling constant $\alpha_c \simeq 0.1$.

The emissivity of NMU and NB processes in the non-superfluid npe matter is usually taken from Friman & Maxwell (1979), in which the one-pion-exchange Born approximation with phenomenological corrections was used for consideration. For the emissivity of QMU and QB processes, we take the results of Iwamoto (1982).

4 COOLING CURVES WITH SPIN DOWN

The traditional standard cooling model is often based on the Tolman-Oppenheimer-Volkoff (TOV) equation of hydrostatic equilibrium (Page et al. 2006; Yakovlev & Pethick 2004). All thermodynamic quantities (neutrino emission luminosity and total heat capacity, etc.) are calculated when the rotational frequency of the stars is zero.

In the present work, we investigate the cooling of hybrid stars with spin-down. The equation of thermal balance has been assumed as spherical symmetry although it may be broken in a rotating star. It is reasonable for slowly rotating stars which could be treated as a perturbation to change their structure and chemical composition (Stejner et al. 2009). We combine the equation of thermal balance with the rotating structure equations of the stars (Kang & Zheng 2007; Hartle 1967) and rewrite the energy equation in the approximation of an isothermal interior (Glen & Sutherland 1980)

$$C_V(T_i, v) \frac{dT_i}{dt} = -L_\nu^\infty(T_i, v) - L_\gamma^\infty(T_s, v), \quad (6)$$

$$C_V(T_i, v) = \int_0^{R(v)} c(r, T) \left(1 - \frac{2M(r)}{r}\right)^{-1/2} 4\pi r^2 dr, \quad (7)$$

$$L_\nu^\infty(T_i, v) = \int_0^{R(v)} \varepsilon(r, T) \left(1 - \frac{2M(r)}{r}\right)^{-1/2} e^{2\Phi} 4\pi r^2 dr, \quad (8)$$

where T_s is the effective surface temperature, $T_i(t) = T(r, t)$ is the redshifted internal temperature; $T(r, t)$ is the local internal temperature of matter, and $\Phi(r)$ is the metric function (describing gravitational redshift) (Yakovlev & Haesel 2003). Furthermore, $L_\nu^\infty(T_i, v)$ and $C_V(T_i, v)$ are the total redshifted neutrino luminosity and the total stellar heat capacity, respectively, which are functions of the rotation frequency v and temperature T ; $c(r, T)$ is the heat capacity per unit volume. $L_\gamma^\infty = 4\pi R^2(v) \sigma T_s^4 (1 - R_g/R)$ is the surface photon luminosity as detected by a distant observer (R_g is the stellar gravitational radius). The effective surface temperature which is detected by a distant observer is $T_s^\infty = T_s \sqrt{1 - R_g/R}$. T_s is obtained from the internal temperature by assuming an envelope model (Gudmundsson et al. 1983; Potekhin et al. 1997). The spin-down of stars is due to the magnetic dipole radiation. The evolution of rotation frequency is given by

$$\frac{dv}{dt} = -\frac{16\pi^2}{3Ic^3} \mu^2 v^3 \sin^2 \theta, \quad (9)$$

where I is the stellar moment of inertia, $\mu = \frac{1}{2} B_m R^3$ is the magnetic dipole moment, and θ is the inclination angle between the magnetic and rotational axes. According to Equations (6) – (9), we can simulate the cooling of hybrid stars during spin-down.

In Figure 3, we present the cooling curves of a $1.6 M_\odot$ rotational hybrid star for different magnetic field strengths ($10^9 - 10^{13}$ G) with bag constant $B = 108 \text{ MeV fm}^{-3}$. We find the cooling curves of the star are different in different magnetic fields, especially for the strong magnetic field cases. As we know, the stronger the magnetic field is, the faster the rotational frequency slows down due to the magnetic dipole radiation; the direct Urca processes are then triggered earlier, which results in rapid cooling in a shorter time. In the cases of weaker fields ($B < 10^{10}$ G), direct Urca processes appear at about the stage of photon cooling, and the effect of magnetic fields is not important at that time.

Using the same model as shown in Figure 3, we show the neutrino emissivity of different reactions as well as the photon luminosity as functions of time and rotational frequency with the magnetic field $B_m = 10^{12}$ G in Figure 4. During the spin-down of the star, deconfined quark matter appears in the core of the star and then QDU reactions are triggered at a spin frequency of $v = 1123$ Hz. From then on, the neutrino emissivity of the direct Urca processes dominate the cooling of the star. For a star of age $10^{1.1} < t < 10^{1.9}$ yr, the QDU reactions provide the most efficient neutrino emissivity. We find that NDU processes are triggered at a spin frequency of $v = 492$ Hz which leads to the rapid increase of neutrino emissivity. The photon emission controls the cooling curves from about $t = 10^5$ yr after birth.

In Figure 5, we plot the cooling curves of hybrid stars for different masses. The results of the rotational model with a magnetic field of $B_m = 10^{11}$ G and the traditional model are both presented in the figure (The per star model includes two cooling curves). The results show that the temperatures of the rotating star model are higher than the transitional static cases, especially for the star which includes NDU reactions (1.6 and $1.7 M_\odot$ stars for a bag constant $B = 108 \text{ MeV fm}^{-3}$, 1.8 and $1.9 M_\odot$ stars for

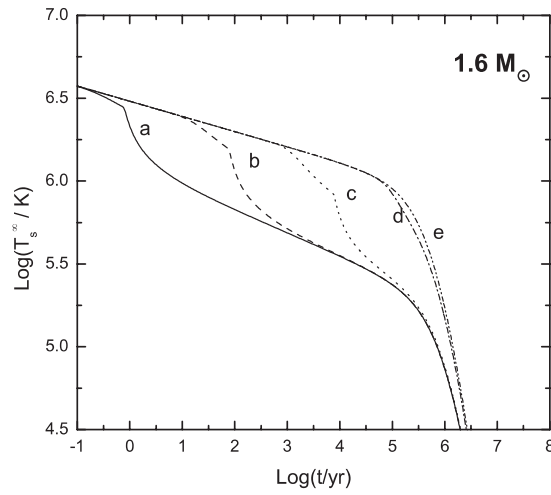


Fig. 3 Cooling curves of a $1.6 M_{\odot}$ rotational hybrid star for various magnetic fields (curve a: 10^{13} G, b: 10^{12} G, c: 10^{11} G, d: 10^{10} G, e: 10^9 G).

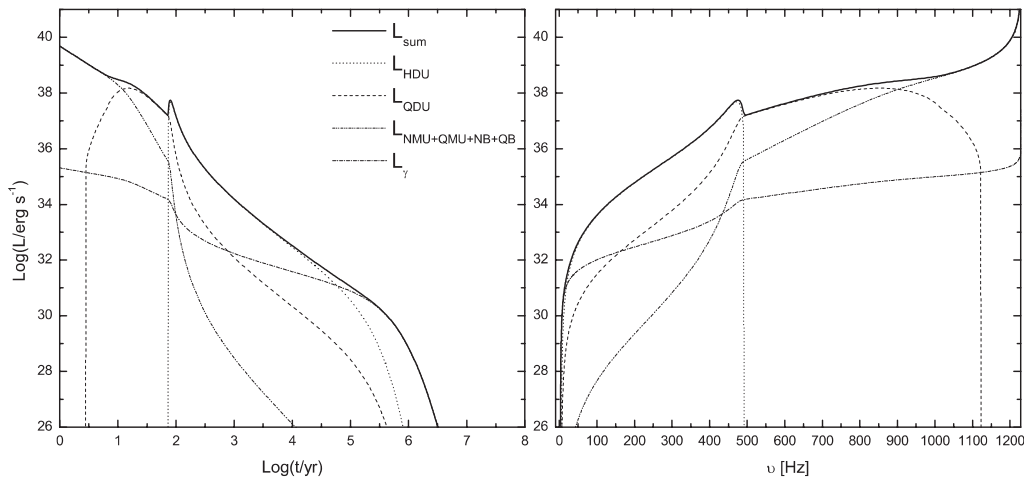


Fig. 4 $1.6 M_{\odot}$ hybrid star with a magnetic field $B_m = 10^{12}$ G for a bag constant equal to 108 MeV fm^{-3} , the neutrino emissivity of different reactions as well as the photon luminosity as functions of time (*left panel*) and rotation frequency (*right panel*).

a bag constant $B = 136 \text{ MeV fm}^{-3}$). As we know, the traditional model uses the equation of hydrostatic equilibrium to study the configuration of stars. The central density of stars and the thermodynamic quantities of neutrino emission luminosity and total heat capacity, etc., are calculated with the rotational frequency of the stars being zero. For the static model, these hybrid stars are born when direct reactions occur. For the rotational model, direct Urca processes appear with the central density gradually increasing during the spin-down of stars, which induces the temperature of the rotating model to be higher than the static model at the stage of neutrino cooling. From Figure 5, we can observe that the cooling curves of some rotating hybrid stars ($1.6 M_{\odot}$ and $1.7 M_{\odot}$ in left panel, $1.8 M_{\odot}$ and $1.9 M_{\odot}$ in right panel) are compatible with the observed data (Page et al. 2004; Weisskopf et al. 2004; Slane et al. 2004), which are

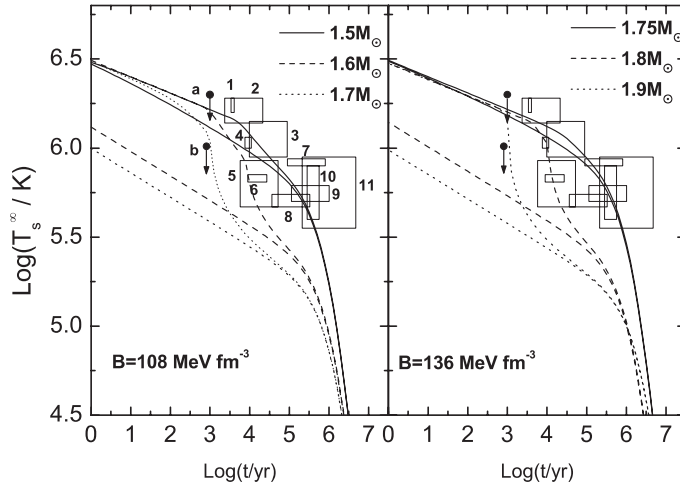


Fig. 5 Cooling curves of hybrid stars for different masses with a magnetic field $B_m = 10^{11}$ G and the cases without rotation. The higher temperature curves correspond to our model for different mass stars. The observational data 1 to 11 are taken from tables 1 and 2 of Page et al. (2004). These stars are: 1. RX J0822–4247, 2. 1E1207.4–5209, 3. PSR 0538+2817, 4. RX J0002+6246, 5. PSR 1706–44, 6. PSR 0833–45, 7. PSR 1055–52, 8. PSR 0656+14, 9. PSR 0633+1748, 10. RX J1856.5–3754, and 11. RX J0720.4–3125. The next two stars, labeled as a and b: a. PSR B0531+21 (Weisskopf et al. 2004), b. PSR J0205+6449 (Slane et al. 2004).

in contradiction with the cooling curves of the transitional model. We find hybrid stars have complicated cooling behaviors during spin-down. For a $M = 1.5 M_\odot$ hybrid star (left panel), the effect of spin-down is weaker than the cases of $M = 1.6 M_\odot$ and $1.7 M_\odot$ because at the interior of a $M = 1.5 M_\odot$ star there only appears QDU reactions, but $M = 1.6 M_\odot$ and $1.7 M_\odot$ stars include QDU and NDU reactions in the process of rotation. Comparing $M = 1.6 M_\odot$ with $1.7 M_\odot$ stars (left panel), we find the earlier appearance of NDU processes that leads to more rapid cooling for the rotating hybrid stars.

We take the value of the bag constant to be relatively large ($B = 108, 136 \text{ MeV fm}^{-3}$) in the paper. Comparing the results for the two parameters, we find that the critical mass of hybrid stars is smaller and the effect of spin-down is more important for the smaller mass hybrid stars with the decrease of the bag constant. In the case of the smaller bag constant, spin-down may lead to larger changes in temperature of the low mass hybrid stars. However, cooling behaviors of hybrid stars for the different bag constants are similar if the changes of the rotational state are similar during the spin-down process.

5 CONCLUSIONS AND DISCUSSIONS

The cooling of hybrid stars with spin-down has been studied in the paper. We combine the cooling equation with the rotational structure equation of stars and simulate the cooling curves of the hybrid stars. The results show that the cooling curves have a clear magnetic field dependence if QDU or/and NDU reactions are triggered during spin-down. The time that direct Urca reactions are triggered controls the occurrence of fast cooling. Comparing the cooling curves of the rotational models with the static models, we find the cooling behaviors of the rotational models are more complicated, and the temperature of the stars is higher, especially when direct Urca reactions appear in the process of rotation. We also find that the cooling curves of some rotational hybrid stars are consistent with the observational data in the case of direct Urca neutrino emission. Through considering the inclusion of superfluidity and superconductivity, we expect that the cooling curves of these rotational hybrid stars can match the pulsar data well in future studies.

It has been studied by many investigators that the different EOS of hadron phase and model parameters of quark phase (bag constant B , coupling constant g) would influence the phase transition densities, rotational structure of hybrid stars and corresponding internal structure, etc. (Schertler et al. 2000; Pan et al. 2006). We will investigate the effect of these parameters on the cooling of rotating hybrid stars in detail.

Acknowledgements This work is supported by the National Natural Science Foundation of China (Grant No. 10747126).

References

- Akmal, A., Pandharipande, V. R., & Ravenhall, D. G. 1998, *Phys. Rev. C*, 58, 1804
Benhar, O., Ferrari, V., Gualtieri, L., & Marassi, S. 2005, *Phys. Rev. D*, 72, 044028
Chubarian, E., Grigorian, H., Poghosyan, G., & Blaschke, D. 2000, *A&A*, 357, 968
De Araujo, J. C. N., De Freitas Pacheco, J. A., Cattani, M., & Horvath, J. E. 1995, *A&A*, 301, 433
Friman, B. L., & Maxwell, O. V. 1979, *ApJ*, 232, 541
Glen, G., & Sutherland, P. 1980, *ApJ*, 239, 671
Glendenning, N. K. 1992, *Phys. Rev. D*, 46, 1274
Glendenning, N. K. 1997, *Compact Stars* (Springer-verlag)
Gudmundsson, E. H., Pethick, C. J., & Epstein, R. I. 1983, *ApJ*, 272, 286.
Hartle, J. B. 1967, *ApJ*, 150, 1005
Hartle, J. B., & Thorne, K. S. 1968, *ApJ*, 153, 807
Iwamoto, N. 1982, *Ann. Phys.*, 141, 1
Kang, M., & Zheng, X. P. 2007, *MNRAS*, 375, 1503
Lattimer, J. M., Prakash, M., Masak, D., & Yahil, A. 1990, *ApJ*, 355, 241
Lattimer, J. M., Prakash, M., Pethick, C. J., & Haensel, P. 1991, *Phys. Rev. Lett.*, 66, 2701
Page, D., Geppert, U., & Weber, F. 2006, *Nucl. Phys. A*, 777, 497
Page, D., Lattimer, J. M., Prakash, M., & Steiner, A. W. 2004, *ApJS*, 155, 623
Pan, N. N., Zheng, X. P., & Li, J. R. 2006, *MNRAS*, 371, 1359
Potekhin, A. Y., Chabrier, G., & Yakovlev, D. G. 1997, *A&A*, 323, 415
Schertler, K., Greiner, C., Schaffner-Bielich, J., & Thoma, M. H. 2000, *Nucl. Phys. A*, 677, 463
Schertler, K., Greiner, C., & Thoma, M. H. 1997, *Nucl. Phys. A*, 616, 659
Slane, P., Helfand, D. J., van der Swaluw, E., & Murray, S. S. 2004, *ApJ*, 616, 403
Stejner, M., Weber, F., & Madsen, J. 2009, *ApJ*, 694, 1019
Weisskopf, M. C., Odell, S. L., Paerels, F., et al. 2004, *ApJ*, 601, 1050
Yakovlev, D. G., & Haensel, P. 2003, *A&A*, 407, 259
Yakovlev, D. G., & Pethick, C. J. 2004, *Ann. Rev. Astron. Astrophys.*, 42, 169